‘Fabrication and Structure of Alginate Gel Incorporating Gold Nanorods

Koji Mitamura,[†] Toyoko Imae,*[,‡] Nagahiro Saito,[†] and Osamu Takai*[,§]

Graduate School of Engineering and Ecotopia Science Institute, Nagoya University, Chikusa, Nagoya 464-8603, Japan, and Graduate School of Science and Technology, Keio University, Hiyoshi, Yokohama 223-8522, Japan

Received: August 23, 2007; In Final Form: October 17, 2007

The gelation of sodium alginate incorporating gold nanorods was investigated. The hybrid gel was obtained by mixing calcium ions with a gel precursor (alginate + nanorod). The gel displayed two plasmon bands in the visible and near-infrared region. The shapes of the hybrid gel grains were controllable, like sphere, ring, and rod. Furthermore, the release of the gold nanorods from the gel phase was observed in a saline solution, accompanying the gel collapse to alginate fibers. Moreover, in the structural investigation of the hybrid gel using small-angle X-ray scattering, it was confirmed that alginate fibers were tightly condensed on the nanorod and formed a shell on it. Such condensation or shell formation resulted from the electrostatic interaction of alginate with hexadecyltrimethylammonium bromide, which protects the nanorods. The hybrid gel retained the same amount of water as the neat gel, although the water content (30 wt %) in a shell on a nanorod was far less than that (98 wt %) of bulk gel.

Introduction

Gold nanorods are worthy of attention due to their anisotropic property originating from their rod shape. Then the nanorods display two absorption bands at visible and near-infrared regions, which are plasmon bands along the short and long axes, respectively.[1] By using this property, the production of near-infrared filters was attempted in a polymer matrix.[2] As another property of gold nanorods, they are fused with each other under irradiation of a strong near-infrared beam, and then thermal energy is generated. This property can be used in medical applications. It was reported that DNA hybridized with gold nanorods was released from the surfaces of rods under the near-infrared beam.[3] Furthermore, there is a report that gold nanorods can kill cancer cells under the near-infrared ray, where the generated heat affects the extinction of the cancer cells.[4] Moreover, the gold nanorods immobilized on a solid substrate were utilized for the recognition of molecules such as an antigen.[5] Thus, the investigations of hybridization with nanorods are spreading in the medical field.

However, since non-biocompatible chemicals such as hexadecyltrimethylammonium bromide (CTAB) are used as protectors in the preparation of gold nanorods, the medical application of gold nanorods cannot sufficiently proceed. Hence, to alleviate the biotoxicity of gold nanorods, the hybridization of gold nanorods with biocompatible materials has been carried out.[6,7] Gold nanorods were coated with biocompatible polyethylene glycol whose terminal was modified by thiol.[6] Furthermore, gold nanorods ware improved by the modification with phosphatidyl choline on their surfaces.[7] Although these surface modification of gold nanorods produced much less damage to living cells than the CTAB-capped nanorods and remarkably increases the biocompatibility of the nanorods, it is still feared that the organic moieties on gold nanorods are digested or decomposed by the immune system or condition changes (pH and ionic strength) in a living body. Such degradation can intensively reduce the medical reaction of the nanorods.

In order to increase efficiently the nanorod migration to cells and the medical reaction of nanorods, it is suggested that the gold nanorods should be encapsulated into biocompatible carriers.[8,9] From such a point of view, the hybridization of the nanorods with hydrogels is preferential, since the rheological property and structure of the hydrogels are responsive to pH, ionic strength, and temperature.[10,11] As such, the hybridization of nanorods with microgels of an artificial poly(*N*-isopropyl acrylamide) (NIPAM) was reported.[12] However, nontoxicities of artificial macromolecules are not necessarily clarified and their use carries a lot of risks without carefully testing for toxicity.

On the other hand, since biomacromolecules, especially edible macromolecules, are less toxic for living bodies, they are suitable to use. Sodium alginate (SA) is a polysaccharide from a sea plant and is utilized as a nontoxic food additive and a water-retentive agent. The alginate is easily gelated by adding dications such as calcium ion.[13] The alginate fibers are cross-linked by coordination bonds between calcium ions and oxygen atoms (−OH and $-COO^-$) on the alginate fibers. From its biocompatible property, alginate gel is applied as a scaffold in the tissue engineering.[14] Another characteristic of arginate gel is moldability, that is, the morphology of the gel can be controlled by the preparation method. The shape-regulated gel can be applied to drug delivery systems, liquid crystal displays,[15] microreactors, and synthesis of materials with unique crystal structures.[16] For example, there are reports on the preparation of spherical microcapsules composed of alginate gel in water-in-oil microemulsions or microfluidic devices with aim of creating drug delivery systems.[17,18]

The hybrid materials of gold nanorods with arginate gel are expected to reduce the toxicity of gold nanorods and to apply as medical materials, retaining the characteristic properties of both alginate gel and gold nanorods. Thus, in this study, as a

* Corresponding authors. T.I.: tel/fax, +81-45-566-1799; e-mail, imae@educ.cc.keio.ac.jp. O.T.: tel/fax, +81−52-789−3259; e-mail: takai@esi.nagoya-u.ac.jp.
[†] Graduate School of Engineering, Nagoya University.
[‡] Keio University.
[§] Ecotopia Science Institute, Nagoya University.

10.1021/jp076755a CCC: $40.75
Published on Web 12/15/2007

new combination, the gelation of SA incorporating gold nanorods was demonstrated, and the moldability of the obtained hybrid gel was tested. In addition, the stability of the hybrid gel in a saline solution was examined. Finally, the structure of the hybrid gel was investigated by small-angle X-ray scattering (SAXS) to reveal the mechanism of the hybridization of gold nanorods with alginate gel and to obtain the structural information on a swollen gel (hydrogel).

Experimental Section

Materials. Tetrachloroauric acid ($HAuCl_4 \cdot 4H_2O$), sodium boronhydride ($NaBH_4$), and silver nitrate ($AgNO_3$) were purchased from Sigma Aldrich. CTAB (MW = 364.5), ascorbic acid, and calcium chloride ($CaCl_2$) were commercially available at Wako Pure Chemical Industries, Ltd. SA was a commercial product from Scientific Polymer Product Inc. All chemicals were used without further purification. Ultrapure water (<0.054 mS) was used throughout as an aqueous medium.

Preparation of Gold Nanorods. Gold nanorods were synthesized via a seed method.[19,20] To prepare a seed solution, an aqueous solution (1.5 cm^3) of 0.25 mM $HAuCl_4$ and 95 mM CTAB was added to a freshly prepared aqueous solution (0.08 cm^3) of 10 mM $NaBH_4$ dropwise under vigorous stirring. Then the solution was colored from yellow to brown. To prepare a growth solution, an aqueous solution (20 cm^3) of 0.25 mM $HAuCl_4$ and 95 mM CTAB was mixed with an aqueous solution (0.16 cm^3) of 10 mM $AgNO_3$ and an aqueous solution (0.15 cm^3) of 0.1 M ascorbic acid with mild stirring. Then the yellow solution changed to transparent. As a next step, the seed solution (0.3 cm^3) was mixed with the growth solution and kept for at least 12 h. Finally, the solution became red. All processes were performed at 30 °C.

Formation of Hybrid Gel. After a gold nanorod dispersion (3.0 cm^3) was centrifuged (at 30 000 rpm for 5 min) to remove excess CTAB, separated precipitates were redispersed in water (3.0 cm^3). After the same process was repeated as for the preparation of a gel precursor, an aqueous solution (0.30 cm^3) of 2.5 wt % SA was added to the nanorod dispersion (3.0 cm^3), and the mixture was stirred for 20 min. The gel was prepared by blending the gel precursor with an aqueous solution (0.23 cm^3) of 0.1 M calcium chloride and keeping for 24 h. The processes were carried out at room temperature (~25 °C).

Measurements. Transmission electron microscopic (TEM) observation was done with a JEM-2500TS microscope. Then an aliquot (5 mm^3) of a dispersion of the as-prepared gold nanorods was dropped on to and dried on a carbon film supported by a copper grid. For TEM observation of an obtained gel, the sample was flaked under sonication (3 h). Optical microscopic observation of the hydrogel was performed on a Nikon Eclipse ME600 microscope. UV−visible−near IR absorption spectrum and transmittance measurements were performed with a Shimazdu UV3600 instrument, using polystyrene cells (1 cm^3 path). SAXS measurements were carried out on a RINT 2000 Nanofinder using a CuKα X-ray source. The scattering intensity was recorded on an imaging plate (IP) at a 1 m camera length (distance between a sample and IP). The sample was sealed between capton films (polyimide films) and exposed with X-ray for 10 h. Background intensity (from only capton films) was taken before each measurement and subtracted from the sample intensity. Gravitometric measurements of water entrapped inside a gel were performed by a weight balance (Mettler AB104-S). Wet gel (after wiping excess water from the surface) was dried for 1 day. The net weight of water was evaluated as a difference between weights of gels before and after drying.

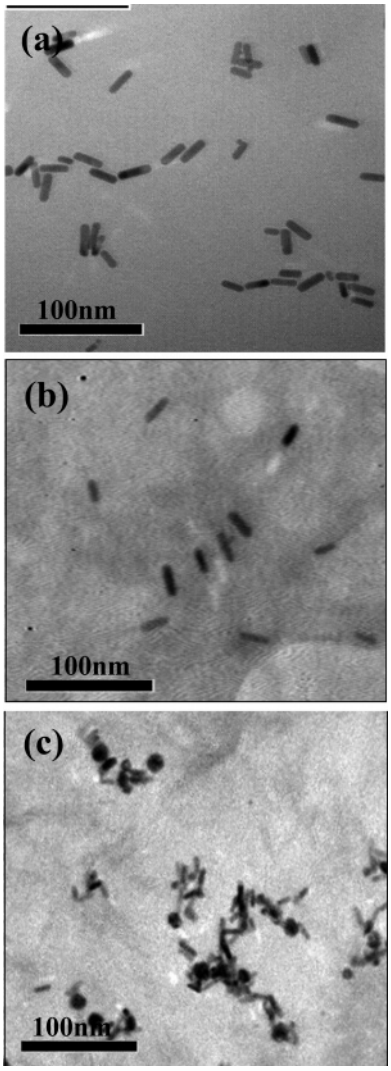

Figure 1. TEM images of (a) as-prepared gold nanorods, (b) hybrid gel, and (c) liquid phase after dialysis of hybrid gel in saline solution.

Results and Discussion

Fabrication of Hybrid Gel. The gold nanorods were prepared via a seed-mediated method, and the excess CTAB was removed in order to avoid the unexpected hybridization between free CTAB and SA. A TEM image of the resultant gold nanorods is shown in Figure 1a. From TEM observation, the nanorods had an average cross-sectional radius of 4.4 ± 0.4 nm and a length of 32.3 ± 2.3 nm, where the aspect ratio is 3.5. When a dispersion of resultant nanorods was mixed with an aqueous solution of SA, the mixture remained red and fluid. However, when this pregel mixture was blended with an aqueous solution of 0.1 M calcium chloride, the gel phase separated. As shown in the optical microscopic images (Figure 2), the obtained gel phase was red, while a neat gel without nanorods was pale yellow. This indicates that the gold nanorods remain in the gels. By the way, $[Ca^{2+}] = 6.55$ mM against $[COO^-$ in SA$] = 12.6$ mM was the minimum calcium concentration at which the liquid phase became completely transparent. Since the positive charge is almost equal to the negative charge at these conditions, it can be indicated that the gelation is completed at the condition where alginate fibers are neutralized by adding calcium ions.

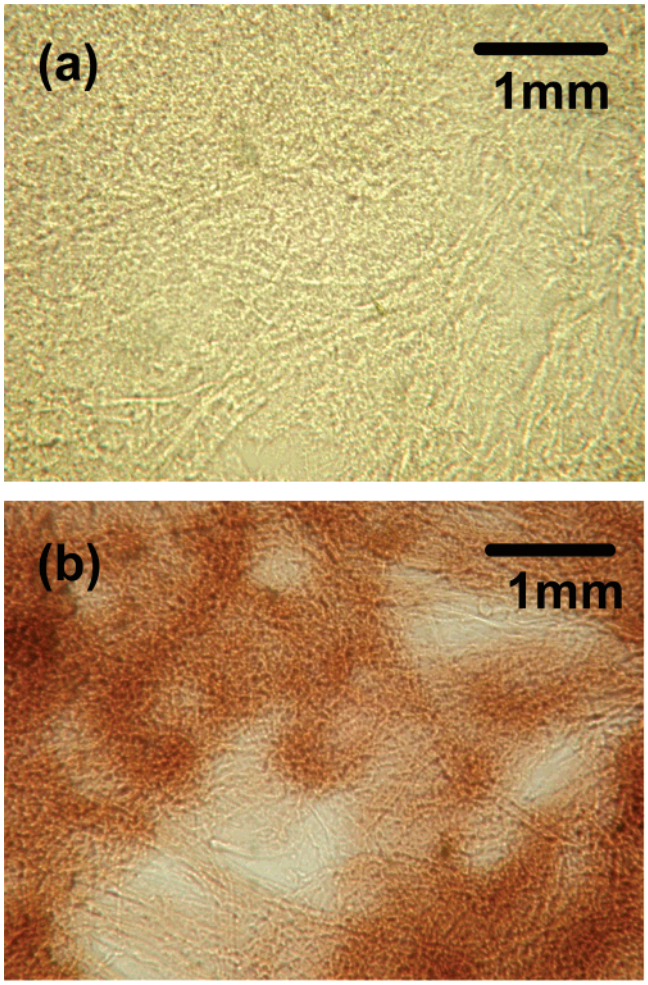

Figure 2. Optical microscopic observation of alginate gels: (a) neat and (b) hybrid.

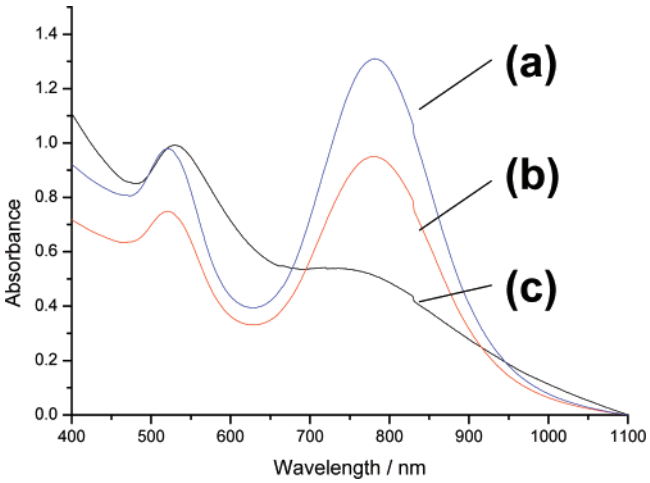

Figure 3. UV−visible−near-infrared absorption spectra of (a) as-prepared gold nanorods, (b) hybrid gel, and (c) liquid phase after dialysis of hybrid gel in saline solution.

The swollen gel displayed two characteristic absorption bands at 524 and 781 nm, as shown in Figure 3b. Similar bands (at 524 and 788 nm) were also observed for as-prepared gold nanorods in an aqueous medium (see Figure 3a), which are originated from the longitudinal and transversal plasmon of gold nanorods, respectively. There is no shift in these bands through the hybridization, indicating no variation in the optical character of gold nanorods. Moreover, as seen in a TEM image (Figure 1b), gold nanorods in random arrangement were dispersed inside

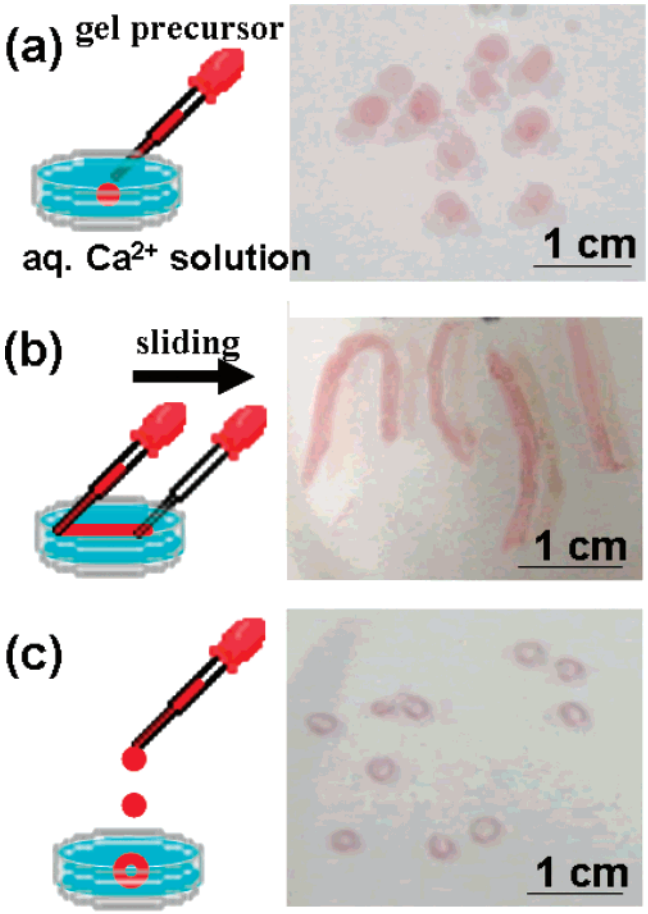

Figure 4. Visual observation of hybrid gels with various shapes: (a) sphere, (b) rod, and (c) ring. The preparation procedure of gel is illustrated at the left of each photograph.

a swollen gel matrix without any coagulation. These spectroscopic and microscopic results directly imply the incorporation of gold nanorods inside the alginate gel matrix.

There is a report on the incorporation of gold nanorods in artificial gel composed of NIPAM.[12] The hybrid NIPAM gel displayed the swelling behavior under irradiation of a strong near-IR ray, while a NIPAM gel showed such behavior by heating. Correspondingly, an alginate gel can be molded in various shapes, depending on the preparation procedures.[21] Since spherical beads of alginate gel are prepared by a simple injection of a gel precursor into an aqueous pool containing calcium ions, the studies of gel particles mainly have focused on spherical architectures.[17,22] On the other hand, formation of other complex shapes such as thread and plate was achieved by using templates and microfluidic devices.[21,23] Since the molded gels are utilized in the application as microreactors or microcapsules for drug delivery systems and scaffolds for cell culture,[14,17] the moldability of the alginate gel after hybridization of gold nanorods is significant to investigate, with expectation that the characteristic functionality can be supplied by gold nanorods in the alginate gel.

In the present preparation, the spherical gel grains were formed, as shown in Figure 4a, when a small amount (~8 mg) of gel precursor was directly injected in an aqueous solution including calcium ions ($[Ca^{2+}] = 0.1$ M). Furthermore, rod-shaped gel was created by a procedure wherein an injection syringe was linearly moved during the injection in an aqueous solution of calcium ions (see Figure 4b). In addition, ring-shaped grains were obtained by dropping a droplet (~8 mg) from 3 cm height above the water level (Figure 4c). These examples

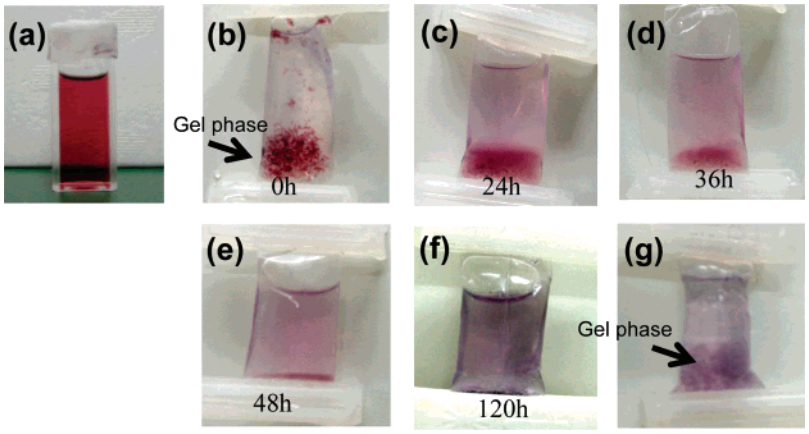

Figure 5. Visual observation of (a) as-prepared gold nanorod dispersion, (b−f) hybrid gel in a saline solution after various hours, and (g) liquid phase of part f after adding calcium ions.

claim that the size and shape of the gel are controllable by the fabrication procedure. Especially, the gel shape can be molded by regulating the diffusion or spread of the gel precursor into an aqueous solution of calcium ions. When the gel precursor is spread isotropically, the gel shape can be spherical. On the other hand, in the condition where the diffusion of the gel precursor is limited in a certain direction, the unique shape of the gel grain is obtained. The linear movement of a syringe and the dropping of the gel precursor are procedures to regulate the spread direction.

The behavior or stability of the hybrid gel in a saline solution was also investigated, since it can be vital for the medical applications. The hybrid gel after 24 h of growth in an aqueous solution of $[Ca^{2+}] = 6.55$ mM was sealed in a dialysis membrane (MWCO = 500) and dialyzed in phosphate-buffered saline solution (pH 7.4, calcium ion free). While as-prepared gold nanorods were dispersed (Figure 5a), the gel phase in saline solution was separated from the transparent liquid phase, as seen in Figure 5b. However, after dialysis for 6 h, the liquid phase, which separated from the gel phase, displayed pale red color (Figure 5c). The color of the liquid phase became obviously strong after 24 h dialysis, and it was purple after further dialysis (120 h), as seen in Figure 5d−f, although the gel phase still remained. The UV−vis−near IR spectrum of the liquid phase (after 120 h) exhibited the characteristic plasmon bands, although the longitudinal plasmon band slightly weakened, as seen in Figure 3c. These results indicate that the gold nanorods were released from the gel phase, and the weakening of longitudinal band was due to the coagulation of gold nanorods upon removing CTAB molecules from the nanorod surface through dialysis. Such coagulation was found by the TEM observation (Figure 1c). It is certainly confirmed from these results that the gold nanorods were released from the gel into a saline solution.

Additionally, the presence of ungelated alginate in the liquid phase after the dialysis for 120 h was confirmed as follows: Calcium ions were added in the excess ion-free liquid phase after dialysis in pure water (without any additive ions). Then a gel phase was generated from the liquid phase, as shown in Figure 5g. This indicates that the alginate fibers were also released from the gel phase in a saline solution. The release of gold nanorods accompanying alginate fibers is due to the disruption of the hybrid gel in a saline solution, since it is known that the alginate gel breaks in a concentrated NaCl solution, where Na^+ ions reduce the cross-linkage of gel fibers by replacing Ca^{2+} ions.[24] The destruction of the gel structure

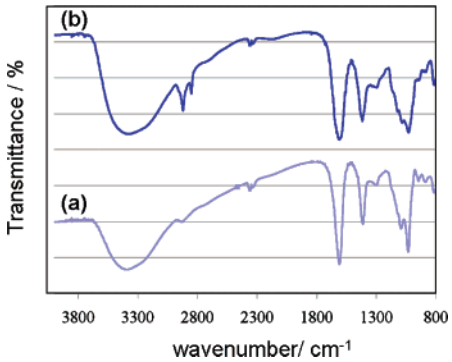

Figure 6. Infrared absorption spectra of (a) alginate gel and (b) hybrid gel.

resulted in the release of gold nanorods from the gel phase and brought about the color development of the liquid phase.

Structure of Hybrid Gel. For the applications using the hybrid gel, it is crucial to confirm how gold nanorods are entrapped in or interact with the alginate gel. In the UV−vis−near IR absorption spectra, the blue shift of the longitudinal plasmon peak (from 788 to 781 nm) upon gelation presumably indicates the change in reflective index of the medium (water and alginate) just surrounding gold nanorods, originating with some interaction (binding) of gold nanorods and alginate gel. Since alginate polymers possess negative charges from COO^- groups and a gold nanorod is positively charged due to the CTAB bilayer on its surface,[7] the interaction is supposed to be an electrostatic one between CTAB-capped gold nanorods and alginate gel.

As an alternative attempt to presume the nature of the interaction in the swollen gel (hydrogel), infrared absorption spectroscopic measurements were performed for the neat and hybrid gels, in order to compare the binding state of alginate with Ca ions and CTAB-capped gold nanorods. There was no difference between the two spectra (Figure 6a,b) at the low wavenumber region, where antisymmetric and symmetric stretching vibration bands of carboxylate (COO^-) were found at 1611 and 1424 cm^{-1}, respectively, indicating no distinguishable variation in the vibrational modes of alginate after gelation. On the other hand, the bands originated from antisymmetric and symmetric vibration modes (2920 and 2848 cm^{-1}, respectively) of methylene ($-CH_2-$) were obviously found in the spectrum of hybrid gel. This result indicates the existence of CTAB molecules inside the gel, since sodium alginate has no $-CH_2-$ groups in its chemical structure.

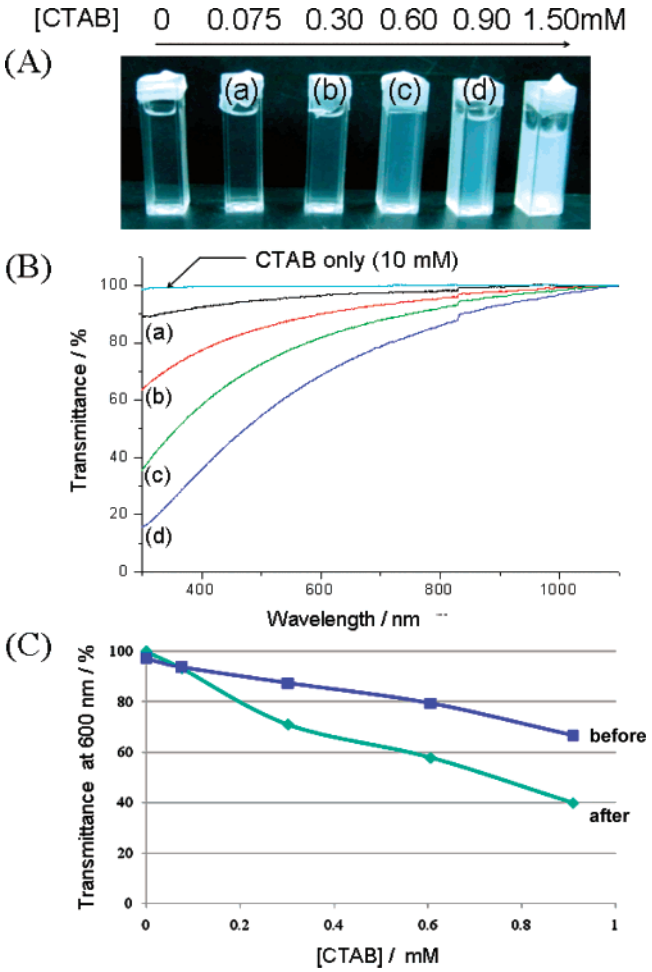

Figure 7. (A) Visual observation of mixtures of sodium alginate with CTAB at various concentrations (0−1.5 mM). (B) Transmittance as a function of wavelength at CTAB concentrations of (a) 0.075, (b) 0.30, (c) 0.60, and (d) 0.90 mM. (C) Transmittance (at 600 nm) as a function of CTAB concentration before and after gelation. In all cases, alginate concentration was 12.6 mM in repeating unit.

Since direct interaction can occur between alginate and CTAB on the hybridization between alginates and CTAB-capped gold nanorods, for the sake of simplicity, the interaction of CTAB molecules with alginate fibers (in the absence of gold nanorods) was investigated from turbidity measurement. When an aqueous solution of alginate (12.6 mM in repeating unit) was mixed with an aqueous solution of CTAB at concentrations of 0, 0.075, 0.3, 0.6, 0.9, 1.5 mM, strong turbidities in the mixtures were visualized with increasing CTAB concentration, as shown in Figure 7A. The turbidities were also quantified by transmittance in UV−vis−near IR spectra as a function of wavelength and CTAB concentration (see Figure 7, parts B and C, respectively). Although an aqueous solution of CTAB itself did not show the turbidity at all, the transmittance of the mixture linearly decreased with CTAB concentration. These results support the formation of aggregates by the interaction between CTAB and alginate. Furthermore, the precipitate was generated at a high CTAB concentration [1.5 mM above the critical micelle concentration (0.92−1.0 mM)],[25] due to an effect of neutralization of electric charges, indicating the strong electrostatic interaction between CTAB and alginate. The turbidity behavior was also observed after gelation (adding calcium ions at 6.55 mM), and the linear decrease in transmittance with CTAB concentration was obtained even in the gel, as seen in Figure 7C, although the decreasing of transmittance was more dominant

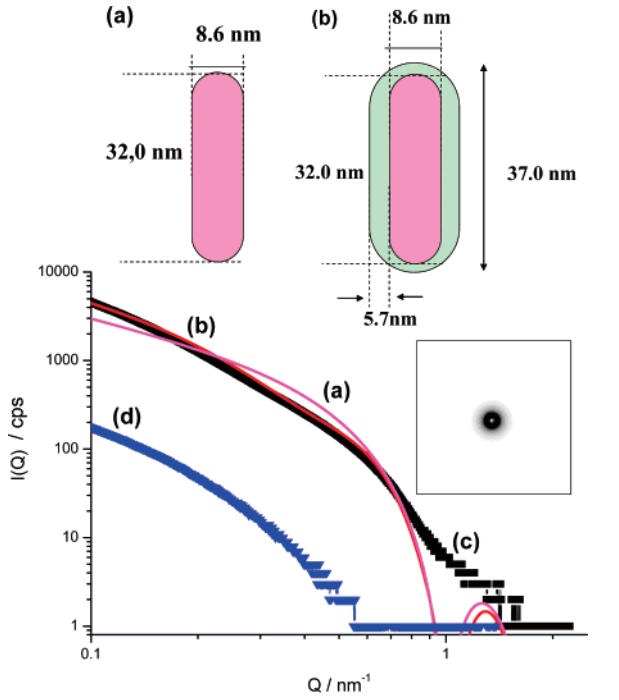

Figure 8. Double logarithmic plots of $I(Q)$ vs Q of alginate gels. Theoretical fitting is based on (a) a bare model and (b) a core−shell model. Experimental data are of (c) hybrid gel and (d) neat gel. Inset is a two-dimensional scattering image.

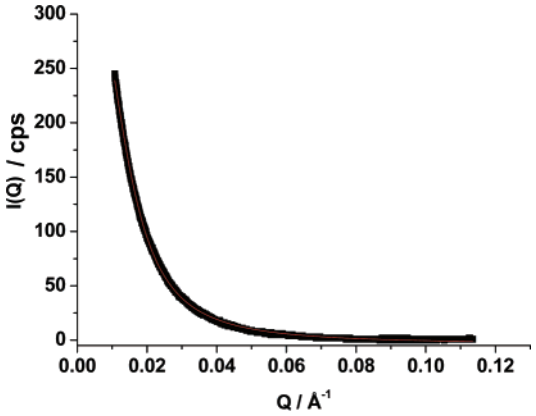

Figure 9. A scattering profile of a neat alginate gel. A red line represents a fitting curve by a Lorenz function.

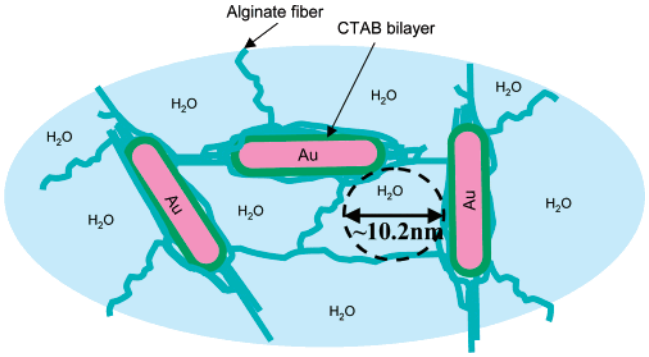

Figure 10. A schematic illustration of hybrid gel structure.

than that before the gelation. It is suggested that the strong interaction remains even in the gel.

Regarding the structural study of a metal particle/polymer hybrid, a core−shell structure of gold nanoparticles in polystyrene or poly(ethylene oxide) matrix was investigated by SAXS.[26] Thus, the SAXS methodology was employed as a tool

for revealing the entrapping mechanism of the alginate gel and clarifying the structure at the vicinity of the gold nanorods in the present work. The hybrid gel was prepared by the method described in the Experimental Section, since homogeneous Ca−alginate gels are prepared by this procedure.[27] The scattering intensity ($I(Q)$)−scattering vector (Q) profiles of neat and hybrid alginate gels are shown in Figure 8. Since both scattering curves monotonically decreased with increasing scattering vector, it is mentioned that the gold nanorods are randomly arranged inside the gel matrix. This fact was also confirmed by the result that a two-dimensional scattering image in Figure 8 (inset) did not show any anisotropic pattern.

As structural evaluation of a neat alginate gel, the blob length (ζ) (based on a de Gennes's scaling theory[28]) of the gel network, namely, the distance between knots in the network, was estimated by fitting the observed curve to the Lorenz function,[29,30] which can be applied for swelling gels, that is,

$$I(Q) = I_0/(1 + \zeta^2 Q^2) \quad (1)$$

where I_0 corresponds to the scattering intensity at zero scattering vector. Incidentally, since the neat gel contained 95.0 ± 2.3 wt % water according to the gravitometric measurement, eq 1 is applicable to the present swollen system. The optimum fitting result was obtained at an average blob length of $\zeta = 10.2$ nm, as shown in Figure 9. The nanorods could not penetrate into the pre-prepared alginate gel, when the gel was immersed into a nanorod dispersion. It is indicated that the densely cross-linked network prevents the doping of nanorods into the gel, since the blob volume is smaller than the volume of a nanorod (32.3 nm length, 4.4 nm radius).

On the other hand, the scattering intensity from alginate gel hybridized with gold nanorods was stronger (more than one order) than that from the neat gel, as seen in Figure 8. It is due to the high electron density of the gold nanorod, since the scattering intensity is proportional to the square of the electron number inside a scattering unit. Thus, since the contribution of intensity from alginate networks in the hybrid gel is negligibly (one order) small, it is supposed that the nanorods are dispersed with random arrangement in a uniform matrix. Then the scattering intensity vs scattering vector profile is adaptive to following equations for randomly arranged rodlike scatterers.[31]

$$I(Q) = k|F(Q)|^2 \quad (2)$$

$$F(Q) = \{(\rho_e - \rho_e^0)V/QL\}^{1/2}\{J_1(QR)/QR\} = F_0(1/QL)^{1/2}\{J_1(QR)/QR\} \quad (3)$$

where k is a proportional constant, $F(Q)$ is a form factor, ρ_e and ρ_e^0 are the electron densities of a nanorod and a matrix, respectively, V is the volume of a nanorod, L and R ($L > R$) are a length and a cross sectional radius of a rod, respectively, $J_1(X)$ is the Bessel function of the first order, and F_0 ($=\{(\rho_e - \rho_e^0)V\}^{1/2}$) is another proportional constant. Here, the variable parameters on the calculation are F_0, L, and R.

In the initial simulation, only the scattering from bare nanorod in the isotropic matrix was considered (a bare model). The obtained optimum geometric parameters of a nanorod were the length of 32.0 nm and the radius of 4.3 nm, as illustrated in Figure 8a. These were consistent with the values (32.3 and 4.4 nm) from TEM. However, as seen in Figure 8, the calculated scattering intensity profile did not agree well with the experimental data. This indicates that the alginate fibers surrounding the nanorod surface must be considered besides bare nanorods.

Thus, in the second simulation, a core−shell model where the nanorod cores are wrapped with alginate fiber shells (see Figure 8b) was taken into account. In this case, the electron densities of the core and shell correspond to gold and alginate fiber, respectively, where the shell density is higher than that of the matrix. For this model, the eq 3 was varied to the following eq 4[32,33]

$$\begin{aligned} F(Q) &= \{(\rho_e^c - \rho_e^s)V_c/QL_c\}^{1/2}\{J_1(QR_c)/QR_c\} + \{(\rho_e^s - \rho_e^0)V_s/QL_s\}^{1/2}\{J_1(QR_s)/QR_s\} \\ &= \{(\rho_e^s - \rho_e^0)V_s\}^{1/2}[(r/QL_c)^{1/2}\{J_1(QR_c)/QR_c\} + (1/QL_s)^{1/2}\{J_1(QR_s)/QR_s\}] \\ &= F_0[(r/QL_c)^{1/2}\{J_1(QR_c)/QR_c\} + (1/QL_s)^{1/2}\{J_1(QR_s)/QR_s\}] \end{aligned} \quad (4)$$

where ρ_e^i is an electron density of core (i = c) or shell (i = s). V_i, L_i, and R_i, respectively, are volume, length, and radius of a gold nanorod without (i = c) or with (i = s) shell. In the eq 4, the term r denotes the ratio $(\rho_e^c - \rho_e^s)V_c/(\rho_e^s - \rho_e^0)V_s$. The parameters L_i, R_i (i = c and s), F_0 ($=\{(\rho_e^s - \rho_e^0)V_s\}^{1/2}$), and r are variables on the computing. Then the fitting curve and the optimum parameters were obtained and shown as Figure 8b. This calculation is more consistent with the experimental data than the initial calculation (a bare model): The evaluated core radius (4.3 nm) and the core length (32.0 nm) are reasonable in comparison with the average size of the nanorods from TEM observation. Meanwhile, the shell thickness was 5.7 nm. Since this is thicker than the bilayer thickness (2.0−3.0 nm) of CTAB coating a gold nanorod, the alginate fibers must be a component of the nanorod shell along with the CTAB bilayer. In the present calculation, the fitting is not enough at a Q range around 1 nm^{-1}, because the polydispersity of the core/shell sizes is not taken into account.

Concerning the analysis of the SAXS curve, the ratio r, besides the structural parameters (R_i and L_i) described above, was obtained from the fitting on the basis of the eq 4. The value was evaluated as 5.5, which is larger than 1.0. The parameter r reflects on the relation of electron densities of matrix, shell, and core. Then the larger value of r declares that the first term in the eq 4, that is, the X-ray scattering from the core, is more dominant. Thus, a ratio r of more than 1.0 indicates that the contribution of the core (gold) for X-ray scattering is higher than that of the shell (alginate fiber).

More detailed information for the gel structure was obtained from the r value as follows: Suppose we describe V_i as a volume of a cylinder with hemispherical caps ($V_i = \pi R_i^2(L_i - 2R_i) + (4\pi/3)R_i^3$, i = c and s). Since it was revealed from gravitometric analysis that the hybrid gel included 98.2 ± 1.2 wt % water, the electron density (330 nm^{-3}) of water was applied as that (ρ_e^0) of the matrix. Furthermore, since the core consists of gold nanorod, the electron density (ρ_e^c) of the core was regarded as that (4.660 nm^{-3}) of gold. Then from the r value (5.5) experimentally obtained, ρ_e^s was obtained as 450 nm^{-3}, which is slightly smaller than that (500 nm^{-3}) of pure alginate but larger than those (330 and ∼340 nm^{-3}) of water and CTA molecule in crystalline CTAB.[34] This calculation supports that the shells on the nanorods consist of 70 wt % alginate fiber and 30 wt % water. Taking the results of the turbidity measurements into account, the result obtained from the SAXS analysis indicates that the alginate fibers are condensed on a gold nanorod shell via the electrostatic attractive interaction with

CTAB; in other words, gold nanorods with a shell consisting of CTAB molecules and alginate fibers were trapped or remained in a network gel of alginate fibers. Thus, the probable structure of the hybrid gel is illustrated in Figure 10. The similarity in water contents (95 and 98 wt %, respectively) between neat and hybrid gels indicates that the blob size of the network in the hybrid gel is similar to that of neat gel, that is, the water retentivity of alginate gel is not degraded through the hybridization with gold nanorods.

The interaction between metal nanoparticles and gelator has been investigated in another report, where silver nanocolloids were hybridized with a low molecular weight gelator and the interaction was clarified by surface enhanced Raman spectroscopy.[35] The interaction shifted or caused the disappearance of the Raman bands. Although spectroscopic measurements were helpful in such an investigation of the interaction, the surrounding structure of the metal nanoparticles was not necessarily confirmed from the spectroscopy. On the other hand, in the present work, the SAXS measurements gave the information on the periphery of gold nanorods. There is no report on the structure of polymer fibers at the vicinity of gold nanorods, except the present report.

Conclusion

In the present work, it was newly reported that gold nanorods were incorporated into alginate gel. The gelation was performed by mixing an aqueous solution of gel precursor (alginate + gold nanorod) with an aqueous solution of calcium ions.

The present work also reported the novel molding method of the hybrid gel grains with various shapes, such as sphere, rod, and ring, by a simple procedure injecting a gel precursor without any template or apparatus. This method makes possible any anisotropic growth of the gel. Such gel grains (including gold nanorods) should be useful as a reaction matrix for the drugs on/in the gel phase with a reactant in a liquid phase, since its surface area is larger than that of the macro gels. Thus, the grains can be used as chemical reactors in the industrial and medical fields.

In saline, the gold nanorods were successfully released from the gel phase, accompanying gel collapse, where gel is again formed by adding calcium ions. Such characteristics of alginate gel in saline solution as well as the moldability of the gel are indispensable and valuable to the versatility of the alginate gel, in application in a living body as capsule and release of drugs in a drug delivery system by controlling the decomposition of the hybrid gel capsule.

The gold nanorods in a hydrogel were densely surrounded by the alginate fibers via electrostatic interaction with CTAB on a gold nanorod. The hybrid gel retained almost the same amount of water as neat alginate gel, even after hybridization of gold nanorods. This indicates the universal status of water retentivity of the gel, although the water content in the vicinity or shell of a nanorod was less than one-third that of the bulk gel.

The characterization of hybrid gels was carried out with microscopes. Additionally, the spectroscopic measurements suggested the possibility of the industrial and medical utilization of the optical character of gold nanorods inside the hybrid gel. SAXS examinations were especially helpful in order to investigate how gold nanorods interact with an alginate gel and are trapped there.

The present work suggested that through the hybridization with an alginate gel, the utilization of gold nanorods could be opened up even in the medical field. In the future, the biocompatibility test of such a gel should be necessary, and further application (such as incorporation of binary doping of drugs with gold nanorods) should be attempted.

Acknowledgment. K.M. is grateful to the 21st century COE program (No. 14COEB01-00 and 14COEB12-00) of Nagoya University for the financial support.

References and Notes

(1) Kim, F.; Song, J. H.; Yang, P. *J. Am. Chem. Soc*. **2002**, *124*, 14316−14317.

(2) Wilson, O.; Wilson, G. J.; Murvaney, P. *Adv. Mater*. **2002**, *14*, 1000−1004.

(3) Chen, C.-C.; Lin, Y-P.; Wang, C.-W.; Tzeng, H.-C.; Wu, C.-H.; Chen, Y.-C.; Chen, C.-P.; Chen, L.-C.; Wu, Y.-C. *J. Am. Chem. Soc*. **2006**, *128*, 3709−3715.

(4) Huang, X.; El-Sayed, I. H.; Qian, W.; El-Sayed, M. A. *J. Am. Chem. Soc*. **2006**, *128*, 2115−2120.

(5) Wang, C.; Ma, Z.; Wang, T.; Su, Z. *Adv. Funct. Mater*. **2006**, *16*, 1673−1678.

(6) Liao, H.; Hafner, J. H. *Chem. Mater*. **2005**, *17*, 4636−4641.

(7) Takahashi, H.; Niidome, Y.; Niidome, T.; Kaneko, K.; Kawasaki, H.; Yamada, S. *Langmuir* **2006**, 22, 2−5.

(8) Gupta, D.; Tator, C. H.; Shoichet, M. S. *Biomaterials* **2006**, *27*, 2370−2379.

(9) Kakinoki, S.; Taguchi, T.; Saito, H.; Tanaka, J.; Tateishi, T. *Eur. J. Pharm. Biopharm.* **2007**, *66*, 383−390.

(10) Raikos, V.; Campbell, L.; Euston, R. S. *Food Hydrocolloids* **2007**, 21, 237−244.

(11) Awad, S. *LWT Food Sci. Technol.* **2007**, 40, 220−224.

(12) Gorelikov, I.; Field, L. M.; Kumacheva, E. *J. Am. Chem. Soc.* **2004**, *126*, 15938−15939.

(13) Zhang, S. M.; Cui, F. Z.; Liao, S. S.; Zhu, Y.; Han, L. *J. Mater. Sci. Mater. Med.* **2003**, *14*, 641−645.

(14) Sakai, S.; Masuhara, H.; Yamada, Y.; Ono, T.; Iijima, H.; Kawakami, K. *J. Biocsci. Bioeng.* **2005**, *100*, 127−129.

(15) Yin, Y.; Xia, Y. *Adv. Mater*. **2001**, *13*, 267- 271.

(16) Zheng, B.; Tice, J. D.; Ismagilov, R. F. *Anal. Chem.* **2004**, *76*, 4977−4982.

(17) Zhu, H.; Srivastava, R.; Brown, J. Q.; McShane, M. J. *Bioconjugate Chem.* **2005**, *16*, 1451−1458.

(18) Sugiura, S.; Oda, T.; Izumida, Y.; Aoyagi, Y.; Satake, M.; Ochiai, A.; Ohkohchi, N.; Nakajima, M. *Biomaterials* **2005**, *26*, 3327−3331.

(19) Sau, T. K.; Murphy, C. J. *Langmuir* **2004**, *20*, 6414−6420.

(20) Mitamura, K.; Imae, T.; Saito, N.; Takai, O. *J. Phys. Chem. B* **2007**, *111*, 8891−8898.

(21) Johansen, A.; Flink, J. M. *Enzyme Microb. Technol.* **1986**, *8*, 145−148.

(22) Nisisako, T.; Torii, T.; Higuchi, T. *Chem. Eng. J.* **2004**, 101, 23−29.

(23) Liu, K.; Ding, H.; Liu, J.; Chen, Y.; Zhao, X. *Langmuir* **2006**, *22*, 9453−9457.

(24) Morris, E. R.; Rees, D. A.; Thom, D.; Boyd, J. *Carbohydr. Res.* **1978**, *66*, 145−154.

(25) Bahri, M. A.; Hoebeke, M.; Grammenos, A.; Delanaye, L.; Vandewalle, N.; Seret, A. *Colloids Surf. A* **2006**, 290, 206−212.

(26) Corbierre, M. K.; Cameron, N. S.; Sutton, M.; Laaziri, K.; Lennox, R. B. *Langmuir* **2005**, *21*, 6063−6072.

(27) Stokke, B. T.; Draget, K. I.; Smidsrød, O.; Yuguchi, Y.; Urakawa, H.; Kajiwara, K. *Macromolecules* **2000**, *33*, 1853−1863.

(28) de Gennes, P. G. *Scaling Concepts in Polymer Physics;* Cornell University: Ithaca, NY, 1979.

(29) Shibayama, M. *Macromol. Chem. Phys.* **1998**, 199, 1−30.

(30) Draget, K. I.; Stokke, B. T.; Yuguchi, Y.; Urakawa, H.; Kajiwara, K. *Biomacromolecules* **2003**, *4*, 1661−1668.

(31) Akiba, I.; Masunaga, H.; Sasaki, K.; Jeong, Y.; Sakurai, K. *Macromolecules* **2004**, *37*, 10047−10051.

(32) Adachi, M.; Harada, T.; Harada, M. *Langmuir* **2000**, *16*, 2376−2384.

(33) Matsumoto, K.; Mazaki, H.; Matsuoka, H. *Macromolecules* **2004**, *37*, 2256−2267.

(34) Solovyov, L. A.; Belousov, O. V.; Dinnebier, R. E.; Shmakov, A. N.; Kirik, S. D. *J. Phys. Chem. B*, **2005**, *109*, 3233−3237.

(35) Miljanić, S.; Frkanec, L.; Biljan, T.; Meić, Z.; Zÿinić, M. *Langmuir* **2006**, *22*, 9079−9081.